


Original Article

Automated Quantitative Image Evaluation of Antigen Retrieval Methods for 17 Antibodies in Placentation and Implantation Diagnostic and Research

Julia Fuchs, Olivia Nonn, Christine Daxboeck, Silvia Groiss, Gerit Moser, Martin Gauster, Ingrid Lang-Olip and Dagmar Brislinger* 

Division of Cell Biology, Histology and Embryology, Gottfried Schatz Research Center, Medical University of Graz, Neue Stiftingtalstraße 6, Graz A-8010, Austria

Abstract

Immunostaining in clinical routine and research highly depends on standardized staining methods and quantitative image analyses. We qualitatively and quantitatively compared antigen retrieval methods (no pretreatment, pretreatment with pepsin, and heat-induced pretreatment with pH 6 or pH 9) for 17 antibodies relevant for placenta and implantation diagnostics and research. Using our newly established, comprehensive automated quantitative image analysis approach, fluorescent signal intensities were evaluated. Automated quantitative image analysis found that 9 out of 17 antibodies needed antigen retrieval to show positive staining. Heat induction proved to be the most efficient form of antigen retrieval. Eight markers stained positive after pepsin digestion, with β -hCG and vWF showing enhanced staining intensities. To avoid the misinterpretation of quantitative image data, the qualitative aspect should always be considered. Results from native placental tissue were compared with sections of a placental invasion model based on thermo-sensitive scaffolds. Immunostaining on placentas *in vitro* leads to new insights into fetal development and maternal pathophysiological pathways, as pregnant women are justifiably excluded from clinical studies. Thus, there is a clear need for the assessment of reliable immunofluorescent staining and pretreatment methods. Our evaluation offers a powerful tool for antibody and pretreatment selection in placental research providing objective and precise results.

Key words: antibody testing, automated quantitative image analysis, enzymatic antigen retrieval, first trimester placenta, immunofluorescence intensity

(Received 26 April 2021; revised 29 July 2021; accepted 13 August 2021)

Introduction

Placentation starts with the implantation of the human embryo into the maternal tissue and thus represents the key for successful pregnancy. Failures in placentation go along with complications in pregnancy such as preeclampsia, intrauterine growth restriction, placenta creta, and gestational trophoblastic disease often resulting in maternal or fetal death (Silva & Serakides, 2016). Methods for the histopathological analysis of implantation abnormalities in clinical routine are limited to lymphocyte infiltration, qualitative analysis of CD163, and hemosiderin staining (Ohyama et al., 2004; Roescher et al., 2014; Liu et al., 2019). Research on implantation abnormalities is reduced to investigations of first to third trimester placentas, as pregnant women are justifiably excluded for ethical reasons. However, immunostaining of placenta sections leads to new insights into fetal development and maternal pathophysiological pathways. In this context, immunostaining not only permits the evaluation of the histological

architecture by preserving the tissue structure, it also enables the assessment of specific protein expression in the context of its microenvironment. However, reliable immunostaining is highly dependent on tissue preparation (Kim et al., 2016).

Whole-slide scanning technologies and automated quantitative image analyses have become standard methods used for histopathological diagnosis in clinics. Importantly, the artificial intelligence of the used programs requires constant training to continuously improve the recognition of specific pathologies (Gurcan et al., 2009; Gertych et al., 2015; Riordan et al., 2015). Hence, antibody staining needs to be consistently and precisely established, and research questions must not deviate from the target recognition of the analysis pipeline (Riordan et al., 2015). In basic research, however, research questions usually differ; hence, existing evaluation pipelines of automated quantitative image analysis programs often lack use. For this reason, conventional histological examinations in basic research, such as investigations of pregnancy-associated diseases and placenta pathologies, are still mainly limited to qualitative analyses, which are subjectively evaluated by the individual (Honig et al., 2005; Gurcan et al., 2009; Higgins, 2015).

Thus, the present study provides a quantitative image analysis pipeline for an unbiased evaluation of fluorescent signal intensities of different antigen retrieval methods for 17 placenta-relevant

*Corresponding author: Dagmar Brislinger, E-mail: dagmar.brislinger@medunigraz.at
Cite this article: Fuchs J, Nonn O, Daxboeck C, Groiss S, Moser G, Gauster M, Lang-Olip I, Brislinger D (2021) Automated Quantitative Image Evaluation of Antigen Retrieval Methods for 17 Antibodies in Placentation and Implantation Diagnostic and Research. *Microsc Microanal* 27, 1506–1517. doi:10.1017/S1431927621012630

antibodies in first trimester placental tissue. We additionally performed conventional qualitative immunostaining analysis to compare the differences in the results of the automated quantitative and qualitative evaluation methods.

Recently, placental organoid cultures and scaffold-based placental barrier and invasion models were developed to study placenta function and pathologies (Aengenheister et al., 2018; Haider et al., 2018; Pemathilaka et al., 2019). Many of these novel placental cell culture models require low-temperature embedding and antigen retrieval methods prior to immunostaining to preserve detailed structures of thermo-sensitive materials, such as biological matrices (Kreuder et al., 2020), membranes of poly(ϵ -caprolactone)/poly(L-lactide) (PCL/PLA) (Vonbrunn et al., 2020), or mRNA (Fuchs et al., 2018). We have already investigated proteolytic pepsin digestion beneficial as an alternative to heat-induced antigen retrieval for thermo-sensitive scaffolds (Fuchs et al., 2018). Hence, the present study also enables us to investigate whether placenta-relevant antibodies positively tested after pepsin digestion on first trimester placenta tissue are applicable to scaffold-based 3D placenta cell culture samples. Based on this, we are able to histologically compare placenta-specific *in vitro* cell culture models to the *in vivo* situation.

Antibodies in the present work were chosen, as they are widely used in characterizing histological structures within placental tissue, both in research and in the diagnosis of placenta pathologies. These include markers detecting general structures as the cytoskeleton (β -actin) (Lanoix et al., 2012), proliferating cells (pC) (Ki-67) (Gauster et al., 2009), vessels [CD31, CD34II, and von Willebrand factor (vWF)] (Kacemi et al., 1999), myofibroblasts in the villous stroma (desmin, vimentin, and SMA) (Kacemi et al., 1999; Sati et al., 2007), as well as markers for structures specific to placental villi such as cytotrophoblasts (CTs) [cytokeratin 7 (CK7), E-Cad, zonula occludens-1 (ZO-1), and alkaline phosphatase placental-like 2 (ALPPL2)] (Marzioni et al., 2001; Nuovo, 2006; Gauster et al., 2009), syncytiotrophoblasts (SCTs) [beta-human chorionic gonadotropin(β -hCG) and leptin] (Londero et al., 2013; Tsai et al., 2015), extravillous trophoblasts (EVTs) [human leukocyte antigen G (HLA-G)] (Guettler et al., 2021), and specific immune cells occurring in the placenta (CD163) (Böckle et al., 2008).

Hence, this study presents a comprehensive quantitative and qualitative analysis of placenta-relevant antibodies. It is intended to be a helpful tool for the selection of pretreatment and antibodies to improve research on placentation and implantation, such as investigations of pregnancy-associated diseases with first and third trimester placental tissues and the analysis of *in vitro* placenta models.

Materials and Methods

Sample Collection

Human first trimester placentas (gestational age: 9–10 weeks) were obtained from women undergoing elective pregnancy termination at the Department of Obstetrics and Gynaecology (Medical University of Graz) or the Femina Med Center (Graz) in accordance with the World Medical Association Declaration of Helsinki. All patients provided written informed consent, and ethical approval was granted by the Medical University of Graz (Nos. 31-019 ex 18/19 and 31-333 ex 18/19). The placental villi used for tissue-specific antibody detection were fixed in 3.7%

paraformaldehyde for 24 h and paraffin-embedded according to standard histological procedures.

Low-Melting Paraffin Embedding of Thermo-Sensitive Electrospun PCL/PLA Scaffolds

Thermo-sensitive electrospun PCL/PLA scaffolds were cultured with first trimester placental villi or the human first trimester trophoblast cell line ACH-3P (Hiden et al., 2007) (a detailed description is provided in Supplementary Materials and Methods). Tissue cultured and cell-seeded scaffolds were fixed in 3.7% paraformaldehyde for 24 h (tissue cultured) or 15 min (cell-seeded) and then dehydrated and embedded by a recently published low-melting paraffin embedding method (Fuchs et al., 2018). Briefly, dehydration and low-melting-point paraffin embedding of fixed samples were performed with the KOS Microwave Multifunctional Tissue Processor (Milestone). Low-melting-point paraffin-embedded tissue-cultured and cell-seeded scaffolds were cut to 7 μ m sections, transferred to SuperFrost Plus™ slides (Thermo Fisher Scientific), and dried overnight at 45°C.

Antigen Retrieval

To standardize immunofluorescent staining of each placental antibody, different antigen retrieval methods were performed on serial sections of first trimester placental villi: (a) no pretreatment, (b) pretreatment with pepsin (Sigma-Aldrich) (Fuchs et al., 2018), (c) heat-induced pretreatment with pH 6 citrate buffer, or (d) heat-induced pretreatment with pH 9 antigen retrieval solution (Leica Biosystems).

Sections included formaldehyde-fixed paraffin-embedded (FFPE) serial sections of first trimester placental villi (5 μ m) and low-melting-paraffin serial sections of PCL/PLA scaffolds cultured with ACH-3P cells or first trimester placental villi. Sections were deparaffinized using Histolab Clear® solution (Histolab®) four times for 5 min each and rehydrated in a graded series of ethanol: 100, 96, 70, and then 50% ethanol, followed by three washes in distilled water for 3 min each.

For enzymatic antigen retrieval with pepsin, slides were incubated with 2 mg/mL pepsin (Sigma-Aldrich) in 0.1M HCl for 30 min at 37°C in a humidified chamber. The digestions were stopped by washing the slides with distilled water for 2 min. Heat-induced antigen retrieval was performed in a Decloaking Chamber (Biocare Medical). The deparaffinized placental villi FFPE sections were completely immersed in antigen retrieval solution or citrate buffer and steamed for 7 min at 120°C. Treated slides were cooled at room temperature for 20 min.

Immunofluorescence of First Trimester Placenta Sections

First trimester placenta sections were washed with 1 \times PBS and blocked with UV Block (Thermo Fisher Scientific) for 10 min. The primary antibody was diluted based on the antigen retrieval pretreatment and datasheet recommendations in antibody diluent (Agilent DAKO) and incubated for 30 min at room temperature. Antibodies used and their dilutions are listed in Table 1. Rabbit (X0936, 15 mg/mL, Agilent Technologies) and mouse (X0931, 0.1 mg/mL, Agilent Technologies) immunoglobulin fractions diluted in antibody diluent according to the highest antibody concentration of the corresponding species used in the study (X0936—noAR: 1:750, pepsin: 1:375, pH6:1:750, pH9:1:750; X0931—noAR: 1:20, pepsin: 1:10, pH6:1:20, pH9:1:20) served as negative controls after the different antigen retrieval methods. Next, slides were washed with 1 \times PBS and incubated with secondary antibody: Alexa Fluor 633-conjugated goat-anti-rabbit or goat-anti-mouse

Table 1. List of Antibodies Used.

Antibody	Origin	Antibody Source*	Code/Clone	Concentration (Stock Solution), mg/mL	Dilution after pretreatment			
					noAR	Pepsin	Steamer pH6	Steamer pH9
ALPPL2	Rabbit	Thermo Fisher Scientific ^a	PA5-22336	1	1:200	1:100	1:200	1:200
β-Actin	Mouse	abcam ^b	AC-15 /ab6276	2.1	1:400	1:200	1:400	1:400
CD 163	Rabbit	DB Biotech ^c	K20-T	2	1:100	1:50	1:100	1:100
CD31	Rabbit	abcam ^b	Ab28364	0.2	1:50	1:25	1:50	1:50
CD34 II	Mouse	Agilent Dako ^d	M7165/QBEnd 10	0.045	1:50	1:25	1:50	1:50
Cytokeratin 7	Rabbit	OriGene Technologies ^e	AP06204PU-N	1	1:200	1:200	1:200	1:200
Cytokeratin 7	Mouse	Thermo Fisher Scientific ^a	OV-TL 12/30	0.2	1:400	1:200	1:400	1:400
Desmin	Mouse	Agilent Dako ^d	M0760/D33	0.111	1:100	1:50	1:100	1:100
E-Cadherin	Rabbit	Cell Signalling Technology ^f	24E10	2.1	1:400	1:200	1:400	1:400
HLA-G	Mouse	Santa Cruz ^g	4H84	0.2	1:100	1:50	1:100	1:100
Ki-67	Mouse	Agilent Dako ^d	M7187	0.45	1:50	1:25	1:50	1:50
Leptin	Mouse	Santa Cruz ^g	sc-48408	0.2	1:50	1:25	1:50	1:50
Smooth muscle actin	Mouse	Agilent Dako ^d	1A4 /M0851	0.071	1:50	1:25	1:50	1:50
β-hCG	Rabbit	Thermo Fisher Scientific ^a	Ab-2 /RB-059-A	0.25	1:100	1:50	1:100	1:100
Vimentin	Mouse	Agilent Dako ^d	V9/M0725	0.156	1:200	1:100	1:200	1:200
vWF	Rabbit	Agilent Dako ^d	F3520	7.0 - 13.0	1:3,000	1:1,000	1:3,000	1:3,000
ZO-1	Rabbit	abcam ^b	ab96587	0.4	1:100	1:50	1:100	1:100

Origin, clone number, and stock concentrations are provided. Primary antibody concentrations used for each antigen retrieval pretreatment of first trimester placental tissue are given. *Headquarters locations of the manufacturers are listed in the Materials and Methods section of Supplementary material. AR, antigen retrieval.

(1:200, Thermo Fisher Scientific, Catalog Nos. A21070 and A21050, detected in the Cy5 channel) for 30 min at room temperature. Finally, slides were washed, and nuclei were counterstained with DAPI for 5 min (1:2,000, Thermo Fisher Scientific). Sections were mounted with ProLongTM Gold Antifade Reagent (Thermo Fisher Scientific). The first section of each series was stained with hematoxylin and eosin to provide a histological overview (Fig. 2, columns a1–h1 and Fig. 3, columns a1–i1).

Immunofluorescence staining was additionally performed on untreated snap-frozen first trimester placenta cryosections to exclude the possibility of nonspecific binding on epitopes occurring through heat or enzymatic digestion and to verify antibody specificity. More detailed information on snap freezing of first trimester placenta tissue, sectioning, and immunostaining is available in the Supplementary Materials and Methods.

Immunofluorescence of Cell-Seeded and Tissue-Cultured PCL/PLA Scaffold Sections

Antibodies showing positive staining on first trimester placental sections after enzymatic antigen retrieval with pepsin (summarized in Supplementary Table 1) were tested on PCL/PLA scaffolds cultured with ACH-3P cells or first trimester placental tissue. Only antibody-relevant proteins that were likely to be

expressed by ACH-3P cells (Hiden et al., 2007) were tested for their antibody binding specificity on PCL/PLA scaffolds (marked in Supplementary Table 1). Cell-seeded and tissue cultured PCL/PLA samples underwent pepsin digestion for antigen retrieval and immunofluorescent staining as described above. Rabbit (X0936, 15 mg/mL, Agilent Technologies) and mouse immunoglobulin fractions (X0931, 0.1 mg/mL, Agilent Technologies) diluted in antibody diluent according to the highest used antibody concentration of the corresponding species (X0936—pepsin: 1:1,500, X0931—pepsin: 1:10) served as negative controls.

Image Acquisition

Images were acquired by scanning 36 tiles at 20× magnification, corresponding to a total area of 6.4 mm² (Fig. 1a), over the same spatial area of all serial sections of the tested antibody. Brightfield and fluorescence images were acquired using the Zeiss Observer.Z1 inverted microscope (Carl Zeiss, Oberkochen, Germany) equipped with the Colibri 7 LED illumination system (Carl Zeiss). For brightfield images, the Axiocam 506 camera (Carl Zeiss) was used, and fluorescence images were taken with the Axiocam 702 mono (Carl Zeiss) equipped with an excitation and emission filter set for the visualization of DAPI, FITC, Cy3, and Cy5. The 20× objective (LD Plan-Neofluar 20×/0.40 corr.,

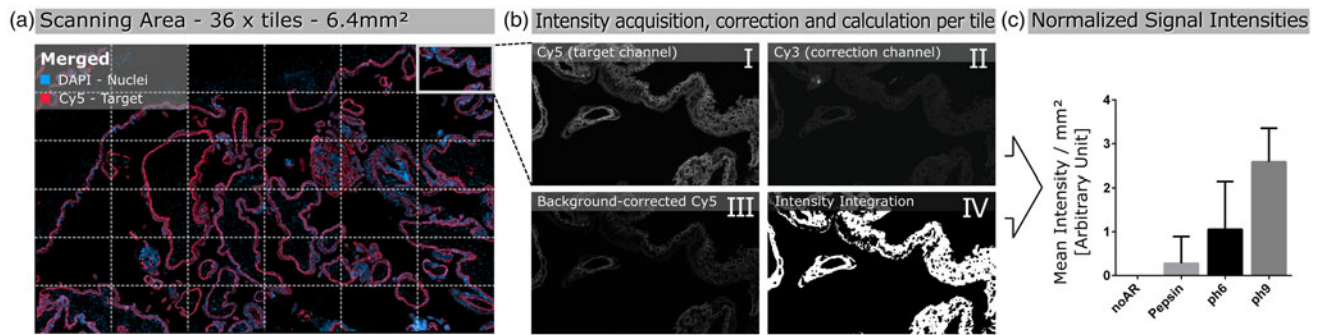


Fig. 1. Schematic illustration of automated quantitative fluorescent image analysis. (a) A 6.4 mm² area resulting from 36 non-overlapping 20 \times images was captured. Images were taken in four fluorescent channels: DAPI, FITC, Cy3, and Cy5 (merged image only shows DAPI and Cy5). (b) Antibody staining fluoresced in the target channel Cy5 (I). Cy3 channel autofluorescence was used as correction (II). Background correction was done by subtracting Cy3 from the target channel Cy5 (III). Using Cy5 image masks (IV) across the background-corrected images, the mean signal intensity over the whole scanning area was calculated in arbitrary units with CellProfiler software. (c) Mean signal intensity was normalized over an area of 1 mm² and plotted for the corresponding pretreatment (the graph displays an example). The analysis (a–c) was conducted for each pretreatment across all 17 antibodies.

$D = 0\text{--}1.5$ mm; Carl Zeiss), and the ZEN 3 blue software (Version 3.0; Carl Zeiss) was used for capturing both the brightfield and fluorescence images.

Quantitative Image Analysis

The Cy5 channel (Fig. 1b-I) exposure time was set using the “Auto Exposure” function on the most intense staining of each antibody out of all different antigen retrieval methods, providing the shortest possible exposure time. The same exposure time was used for all antigen retrieval treatments for each antibody to enable comparison of the fluorescence intensities within a group. A constant exposure time was used for FITC and CY3 channels (Fig. 1b-II) to detect background fluorescence.

We used the open-source cell image analysis software CellProfiler (version 3.1.8; McQuin et al., 2018) to evaluate the mean signal intensity of the Cy5 channel over the entire 6.4 mm² region corresponding to ~ 2.7 billion pixels (Fig. 1a). Specific, positive antibody staining exclusively appears in the wavelength range that corresponds to the fluorophores conjugated to the secondary antibody (Weibrecht et al., 2013). Signals detected in multiple channels were classified as false-positive and, therefore, nonspecific staining. To exclude false-positive signals from the analysis, the Cy3 channel was subtracted from the Cy5 channel (Fig. 1b-III). Additionally, existing background noise was eliminated by using a threshold to improve the signal-to-background ratio (Fig. 1b-IV). Mean signal intensities were normalized across a 1 mm² area and plotted for the respective pretreatments for each antibody (Fig. 1c). More detailed information on the custom-designed CellProfiler pipeline is available in Supplementary Materials and Methods. Calculations and detailed values of the quantitative image analysis are given in Supplementary Table 2.

Morphological Analysis

In addition to the automated quantitative image analysis, immunofluorescent staining of first trimester placenta was qualitatively evaluated. The histological classification of various cell types occurring in first trimester placentas was performed regarding the specific staining reaction pattern and the presence of nonspecific background for each antibody. Positive antibody staining was counted as specific when the fluorescence signal exclusively appeared in the wavelength range corresponding to the fluorophores conjugated to the secondary antibody. Signals appearing

in multiple channels were classified as nonspecific staining. Individual cell types including CTs, SCTs, endothelial cells (ECs), EVT, fibroblasts (Fib), smooth muscle cells, Hofbauer cells, and pC were evaluated. Additionally, a classification category for nonspecific staining was introduced, marked in red to classify irregular and insufficient antibody staining all over the tissue. Green coloring was used to mark specific staining pattern. An intensity grading system was applied, using “-” for negative staining, “○” to display a positive staining reaction, and “●” indicating the cell type that appears the brightest within an antigen retrieval group all over the tissue (if there are intensity differences between cell types). “⊙” marks cell types that show a brighter signal in only some parts of the tissue compared to other positive stained cell types within an antigen retrieval treatment group. Results of the qualitative evaluation are shown in Figure 4.

Statistical Analyses

Mean intensities resulting from the automated quantitative image analysis were statistically evaluated using GraphPad PRISM software (version 6.01). Outliers were identified using the ROUT test with a Q value of 1% (Motulsky & Brown, 2006). Cleaned data were used for further analysis. Data were tested for Gaussian distribution with a Kolmogorov–Smirnov test. Mean fluorescence intensities of the Cy5 signal of all antigen retrieval methods were compared using one-way ANOVA with Tukey’s multiple comparison test. Results were considered statistically significant when $p < 0.05$ (* $p < 0.05$, ** $p < 0.01$, *** $p < 0.001$, and **** $p < 0.0001$).

Results

Automated Quantitative Image Analysis Revealed Differences in Immunofluorescent Intensities Based on the Selected Antigen Retrieval Method

Automated quantitative image analysis revealed that 9 out of 17 tested antibodies required antigen retrieval for immunofluorescent staining (Figs. 2, 3). Antibodies specific for CK7 (rabbit), E-cadherin, vWF, ZO-1, CD31, HLA-G, Ki-67, leptin, and CD163 needed selected pretreatments to stain positive for their antigen. However, β -Actin, desmin, smooth muscle actin (SMA), vimentin, ALPPL2, β -hCG, CD34II, and CK7 (mouse) showed specific immunofluorescent signals without any antigen retrieval pretreatment.

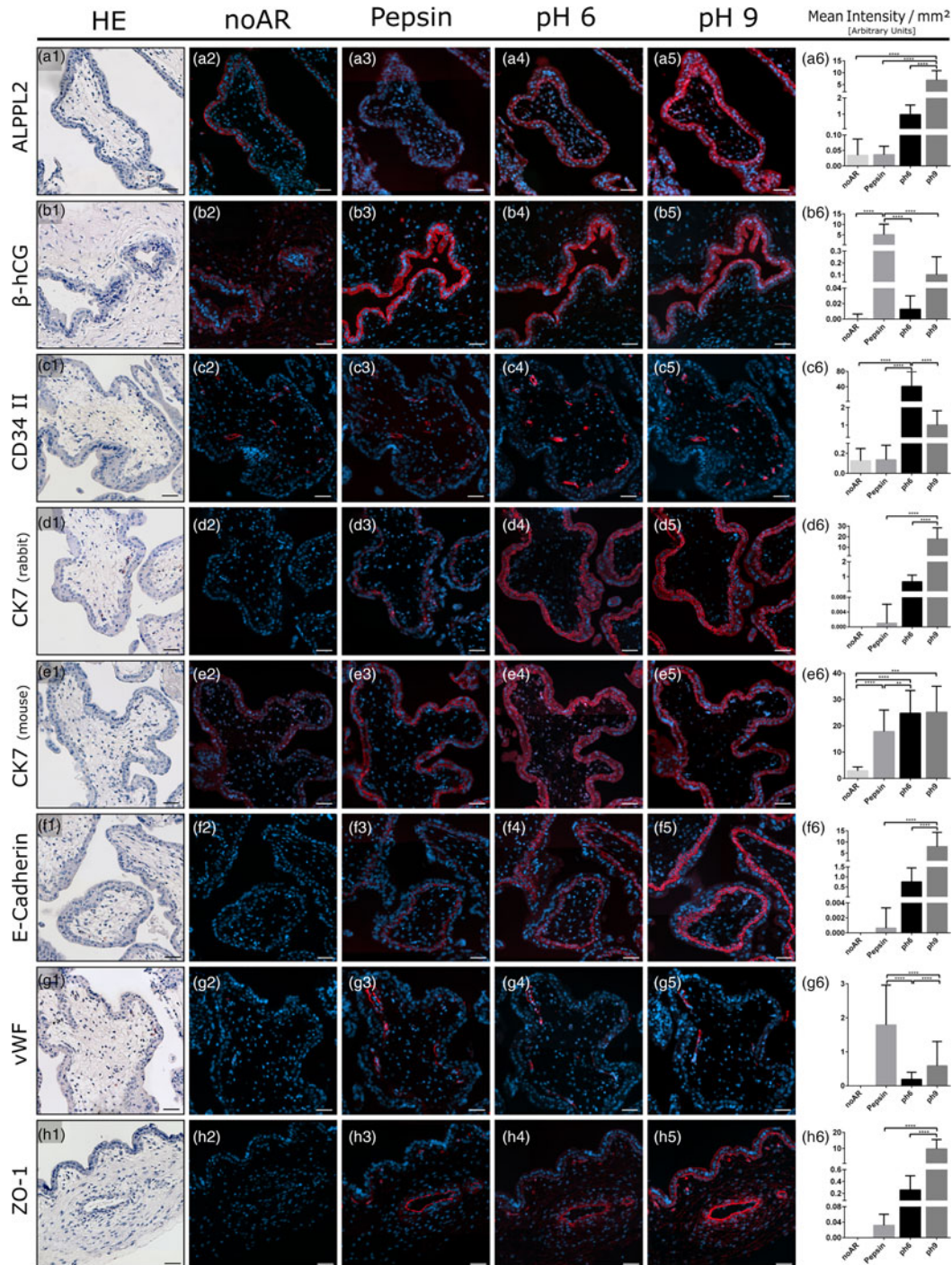


Fig. 2. Immunostaining after different antigen retrieval pretreatments on first trimester placenta serial sections. Antibodies tested show specific binding after enzymatic digestion with pepsin. Hematoxylin and eosin staining (columns **a1–h1**) provides a morphological overview of the tissue. Each of the fluorescent-stained serial sections was treated using one of the different methods: none, pepsin digestion, pH 6 heat-induced epitope retrieval, or pH 9 heat-induced epitope retrieval. Columns 2–5 show representative image details of antibody-stained serial sections after the different pretreatments. The mean fluorescence intensity of the target per mm² evaluated by quantitative automated image analysis is given in the bar chart for each pretreatment (columns **a6–h6**). β-hCG (**b3, b6**) and vWF (**g3, g6**) show significantly improved staining after pepsin digestion. Detailed values of the quantitative image analysis are given in Supplementary Table 2. Scale bars represent 50 μm. noAR, no antigen retrieval; pepsin, enzymatic digestion with pepsin; pH 6, heat-induced epitope retrieval with pH 6 citrate buffer; pH 9, heat-induced epitope retrieval with pH 9 antigen retrieval buffer.

We found heat induction to be the most efficient form of antigen retrieval, followed by enzymatic digestion. Heat-induced antigen retrieval was strongly influenced by the pH value. Four of the antibodies examined, CD34II (Figs. 2c4, 2c6), CD31 (Figs. 3b4, 3b6), leptin (Figs. 3f4, 3f6), and CD163 (Figs. 3i4, 3i6), displayed

the most intense staining after heat-induced antigen retrieval with pH 6. Eleven placenta-specific antibodies, ALPPL2 (Figs. 2a5, 2a6), CK7 (rabbit; Figs. 2d5, 2d6), CK7 (mouse; Figs. 2e5, 2e6), E-cadherin (Figs. 2f5, 2f6), ZO-1 (Figs. 2h5, 2h6), β-Actin (Figs. 3a5, 3a6), desmin (Figs. 3c5, 3c6), HLA-G (Figs. 3d5, 3d6),

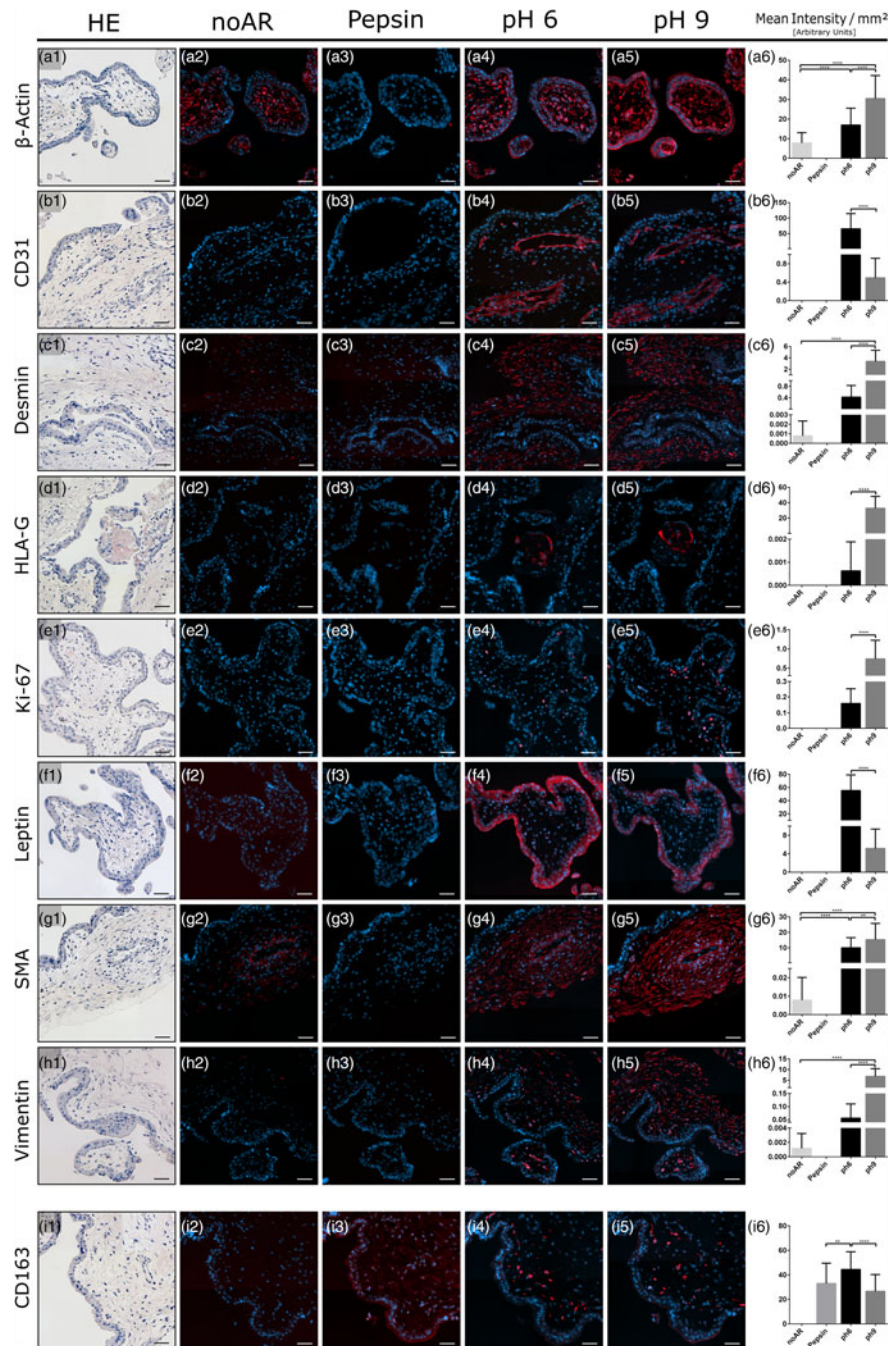


Fig. 3. Immunostaining after different antigen retrieval pretreatments on first trimester placenta serial sections. Tested antibodies show no specific staining after enzymatic pepsin digestion. Hematoxylin and eosin staining (columns a1–i1) provides a morphological overview of the tissue. Each of the fluorescent-stained serial sections was treated using one of the different methods: none, pepsin digestion, pH 6 heat-induced epitope retrieval, or pH 9 heat-induced epitope retrieval. Columns 2–5 show representative image details of antibody-stained serial sections after the different pretreatments. The mean fluorescence intensity of the target per mm² evaluated by quantitative automated image analysis is given in the bar chart for each pretreatment (columns a6–i6). Anti-CD163 was the only antibody (i3) displaying nonspecific staining over the entire tissue after pepsin digestion. Detailed values of the quantitative image analysis are given in Supplementary Table 2. Scale bars represent 50 μm. noAR, no antigen retrieval; pepsin, enzymatic digestion with pepsin; pH 6, heat-induced epitope retrieval with pH 6 citrate buffer; pH 9, heat-induced epitope retrieval with pH 9 antigen retrieval buffer.

Ki-67 (Figs. 3e5, 3e6), SMA (Figs. 3g5, 3g6), and vimentin (Figs. 3h5, 3h6), showed the most intense staining after pretreatment with pH 9.

Enzymatic antigen retrieval with pepsin yielded the brightest signals for β-hCG (Figs. 2b3, 2b6) and vWF (Figs. 2g3, 2g6).

Overall, pretreatment for antigen retrieval was necessary to get the highest signal intensities of selected antibody within its group.

Negative controls (rabbit and mouse immunoglobulin fractions) showed no expression of the antibodies used. Images are shown in Supplementary Figures 2a1–2a4 and 2b1–2b4.

	noAR								Pepsin								ph6								ph9							
	CT	SCT	EC	EVT	Fib	SMC	HBC	pC	CT	SCT	EC	EVT	Fib	SMC	HBC	pC	CT	SCT	EC	EVT	Fib	SMC	HBC	pC	CT	SCT	EC	EVT	Fib	SMC	HBC	pC
ALPPL2	○	○	-	-	-	-	-	-	-	○	-	-	-	-	-	-	●	○	-	-	-	-	-	-	●	○	-	-	-	-	-	-
β-Actin	○	○	○	○	●	○	○	-	-	-	-	-	-	-	-	-	○	○	○	○	●	○	○	-	○	○	○	○	○	○	○	-
β-HCG	●	○	-	-	-	-	-	-	-	○	-	-	-	-	-	-	-	○	-	-	-	-	-	-	-	○	-	-	-	-	-	-
CD 163	-	-	-	-	-	-	-	-	○	○	○	○	○	○	○	○	-	-	-	-	-	-	-	-	-	-	-	-	-	-	-	-
CD31	-	-	-	-	-	-	-	-	-	-	-	-	-	-	-	-	-	○	-	-	-	-	-	-	-	○	-	-	-	-	-	-
CD34 II	-	-	○	-	-	-	-	-	-	-	○	-	-	-	-	-	-	-	○	-	-	-	-	-	-	-	○	-	-	-	-	-
Cytokeratin 7 (rabbit)	-	-	-	-	-	-	-	-	○	-	-	-	-	-	-	-	○	○	-	-	-	-	-	-	○	○	-	-	-	-	-	-
Cytokeratin 7(mouse)	○	○	-	-	-	-	-	-	●	○	-	-	-	-	-	-	○	○	-	-	-	-	-	-	○	○	-	-	-	-	-	-
Desmin	-	-	-	-	○	-	-	-	-	-	-	-	-	-	-	-	-	-	-	-	○	-	-	-	-	-	-	-	○	-	-	-
E-Cadherin	-	-	-	-	-	-	-	-	○	-	-	-	-	-	-	-	○	-	-	-	-	-	-	-	○	-	-	-	-	-	-	-
HLA-G	-	-	-	-	-	-	-	-	-	-	-	-	-	-	-	-	-	-	○	-	-	-	-	-	-	-	○	-	-	-	-	-
Ki-67	-	-	-	-	-	-	-	-	-	-	-	-	-	-	-	-	-	-	-	-	-	-	-	○	-	-	-	-	-	-	-	-
Leptin	-	-	-	-	-	-	-	-	-	-	-	-	-	-	-	-	-	-	-	-	-	-	-	-	-	-	-	-	-	-	-	-
Smooth Muscle Actin	-	-	-	-	○	-	-	-	-	-	-	-	-	-	-	-	-	○	-	-	○	-	-	-	-	○	-	-	○	-	-	-
Vimentin	-	-	-	-	○	-	-	-	-	-	-	-	-	-	-	-	-	-	-	-	-	-	-	-	-	-	-	-	○	-	-	-
vWF	-	-	-	-	-	-	-	-	-	-	○	-	-	-	-	-	-	-	○	-	-	-	-	-	-	-	○	-	-	-	-	-
ZO-1	-	-	-	-	-	-	-	-	-	-	○	-	-	-	-	-	-	-	○	-	○	-	-	-	○	○	●	-	-	-	-	-

Fig. 4. Qualitative evaluation of antibody staining of different cell types in first trimester placenta after different antigen retrieval pretreatments. - indicates no staining, red indicates nonspecific staining, green indicates specific staining. ○ marks cell types that shows positive staining within an antigen retrieval group. ● marks the cell type that show the most intense staining compared to other positive cell types within an antigen retrieval group. ● marks cell types that show more intense staining in some parts of the tissue compared to other stained cell types within an antigen retrieval group. noAR, no antigen retrieval; CT, cytotrophoblast; SCT, syncytiotrophoblast; EC, endothelial cells; EVT, extravillous trophoblast; Fib, fibroblasts; SMC, smooth muscle cells; HBC, Hofbauer cells; pC, proliferating cells.

Antibody Binding Specificity Is Influenced by the Antigen Retrieval Method

We used first trimester placental tissue to investigate the influence of antigen retrieval on antibody binding specificity. Qualitative assessment clearly demonstrated that the method of antigen retrieval had implications for antibody binding specificity and signal intensities (Fig. 4). In some cases, e.g. CK7 antibodies, the determination of cell-type specificity was not possible, since intense staining was frequently observed in two cell types over large areas.

Pretreatment with Pepsin Increased Staining Intensities of β-hCG and vWF Antibodies

All examined antibodies displaying successful staining after enzymatic antigen retrieval with pepsin are illustrated in Figure 2. The quantitative image analysis of the immunofluorescent staining of β-hCG and vWF after pepsin digestion showed significantly higher mean fluorescent signal intensities compared to all other antigen retrieval methods (Figs. 2b6, 2g6), corresponding to the qualitative evaluation (Fig. 4).

CD163 Showed Nonspecific Staining after Enzymatic Antigen Retrieval

While the enzymatic digestion with pepsin improved the staining intensity and/or specificity of certain antibodies, other epitopes were completely degraded, preventing antibody binding. As shown in Figure 3 (columns a3–h3), eight antibodies completely lacked staining after pepsin pretreatment. Anti-CD163 was the only antibody (Fig. 3i3) displaying nonspecific staining over the entire tissue after pepsin digestion.

ACH-3P Cells Cultured on PCL/PLA Scaffolds Stained Positive after Enzymatic Antigen Retrieval with Pepsin

The ACH-3P cell line was generated by fusing first trimester trophoblasts to the choriocarcinoma cell line AC1-1. As such, it is

characterized by the expression of proteins specific for EVT's (Hiden et al., 2007). Only proteins known to be expressed by trophoblast cells as β-Actin, CK7 (rabbit and mouse origins), E-cadherin, and ZO-1 were tested on these sections (see Supplementary Table 1).

Positive staining after enzymatic antigen retrieval with pepsin was obtained after staining for β-hCG, CK7 (rabbit and mouse origins), E-cadherin, and ZO-1 (Fig. 5). Qualitatively, β-hCG (Figs. 5a, 5b) and ZO-1 (Figs. 5i, 5j) showed moderate staining, while high staining intensities were observed for CK7 (rabbit; Figs. 5c, 5d), CK7 (mouse; Figs. 5e, 5f), and E-cadherin (Figs. 5g, 5h). The mouse-origin anti-CK7 antibody showed more consistent staining and improved morphological cell integrity on PCL/PLA scaffolds cultured with ACH-3P compared to the rabbit-origin anti-CK7 antibody. Rabbit and mouse immunoglobulin fractions showed no staining of the antibodies used.

Positive Staining of Endothelial and Trophoblast Cells of First Trimester Placental Villi Cultured on PCL/PLA Scaffolds Was Observed after Pepsin Digestion

To test the applicability of the enzyme-based immunostaining protocol for thermo-sensitive samples, first trimester placental villi cultured on PCL/PLA scaffolds underwent enzymatic antigen retrieval with pepsin and antibody staining. All antibodies tested on these samples showed positive immunostaining.

The anti-CD34II antibody displayed specific staining of EC, marking blood vessels in the villous stroma (Figs. 6a, 6b). Positive signals of the anti-ALPPL2 antibody were observed exclusively in SCT cells and migrated EVT's (Figs. 6c, 6d). Both rabbit- and mouse-origin anti-CK7 antibodies positively stained scaffold-attached first trimester placental villi. Qualitatively, the mouse-origin anti-CK7 antibody (Figs. 6g, 6h) showed brighter and more distinct fluorescence compared to the rabbit-origin anti-CK7 antibody (Figs. 6e, 6f), which displayed impaired morphological cell integrity. However, both antibodies positively recognized EVT's within the PCL/PLA scaffold.

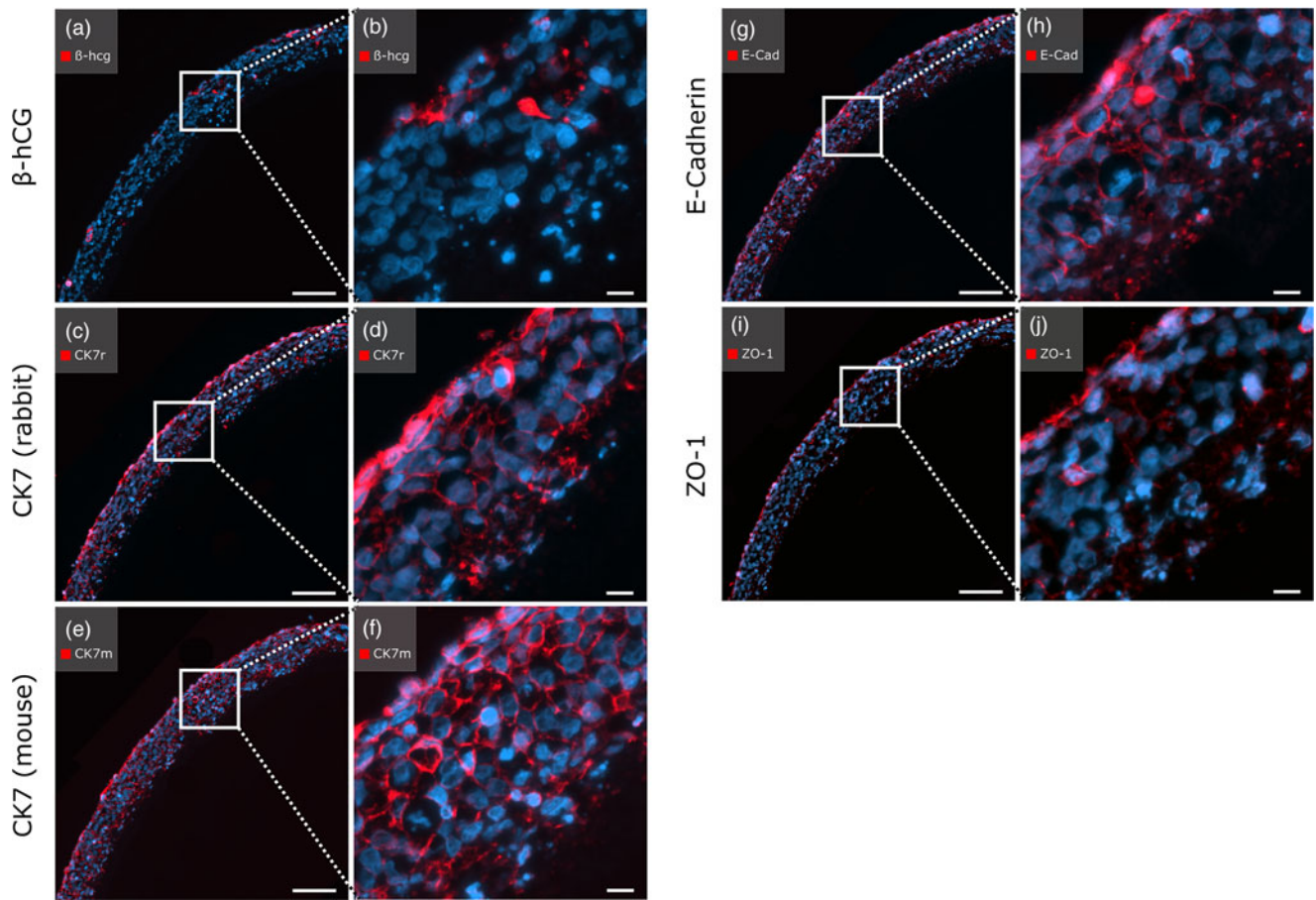


Fig. 5. Antibody staining of the human first trimester trophoblast cell line ACH-3P cultured on heat-sensitive PCL/PLA with placenta-relevant antibodies after pepsin digestion. White boxes indicate the zoom-in area on the right image side. All antibodies tested showed specific fluorescence signals. Scale bars in (a,c,e,g,i,k,m,o) represent 100 μm , and those in (b,d,f,h,j,l,n,p) represent 20 μm .

In addition, positive staining was observed for the transmembrane protein E-cadherin. Both the CT cells and the migrating EVT cells showed positive fluorescence (Figs. 6i, 6j). As expected, SCTs were positive for β -hCG, as were migrated EVTs within the membrane (Figs. 6k, 6l). The endothelial marker vWF displayed positive staining specifically on EC marking blood vessels within the villous stroma. EVTs that migrated through the PCL/PLA scaffold appeared negative for vWF (Figs. 6m, 6n). Anti-ZO-1 antibody showed positive staining with specific fluorescent signals of several cell types, including ECs, CTs, SCTs, EVTs, and F (Figs. 6o, 6p). Rabbit and mouse immunoglobulin fractions showed no expression of the antibodies used (Supplementary Figs. 2c1, 2c2).

Pepsin Digest Serves as Heatless Antigen Retrieval Alternative for Placenta-Relevant Antibodies on Scaffold-Based Placental Cell Culture Samples

All antibodies positively tested after pepsin digestion on first trimester placenta tissue (Fig. 2, columns a3–h3) showed positive immunostaining on tissue cultured PCL/PLA samples after enzymatic antigen retrieval (Fig. 6). In addition, all antibodies expected to be expressed by the ACH-3P cell line displayed positive fluorescence signals on ACH-3P cultured PCL/PLA samples after enzymatic antigen retrieval (Fig. 5).

Immunofluorescent Staining of Snap-Frozen First Trimester Placenta Cryosections without Antigen Retrieval Verifies Antibody Specificity

To exclude nonspecific binding due to heat or enzymatic antigen retrieval, antibodies were additionally tested on first trimester placental cryosections without antigen retrieval. All tested antibodies showed positive immunostaining on the expected cell types and morphological structures in accordance with the references of the literature search (Supplementary Fig. 1; Supplementary Table 3). The comparison of the immunostaining on untreated cryosections with the staining on heat or enzymatically treated paraffin sections allowed the detection or exclusion of nonspecific binding after antigen retrieval and thus the verification of binding specificity. Comparing the results in a qualitative way, no nonspecific antibody binding could be detected after immunostaining on antigen retrieval treated sections. Negative controls (rabbit and mouse immunoglobulin fractions) showed no expression of the antibodies used (Supplementary Figs. 1o, 1p).

Discussion

In this study, we present an evaluation of antigen retrieval methods for 17 antibodies widely used in placental and implantation diagnostic and research. We established an automated quantitative image analysis method for the quantification of

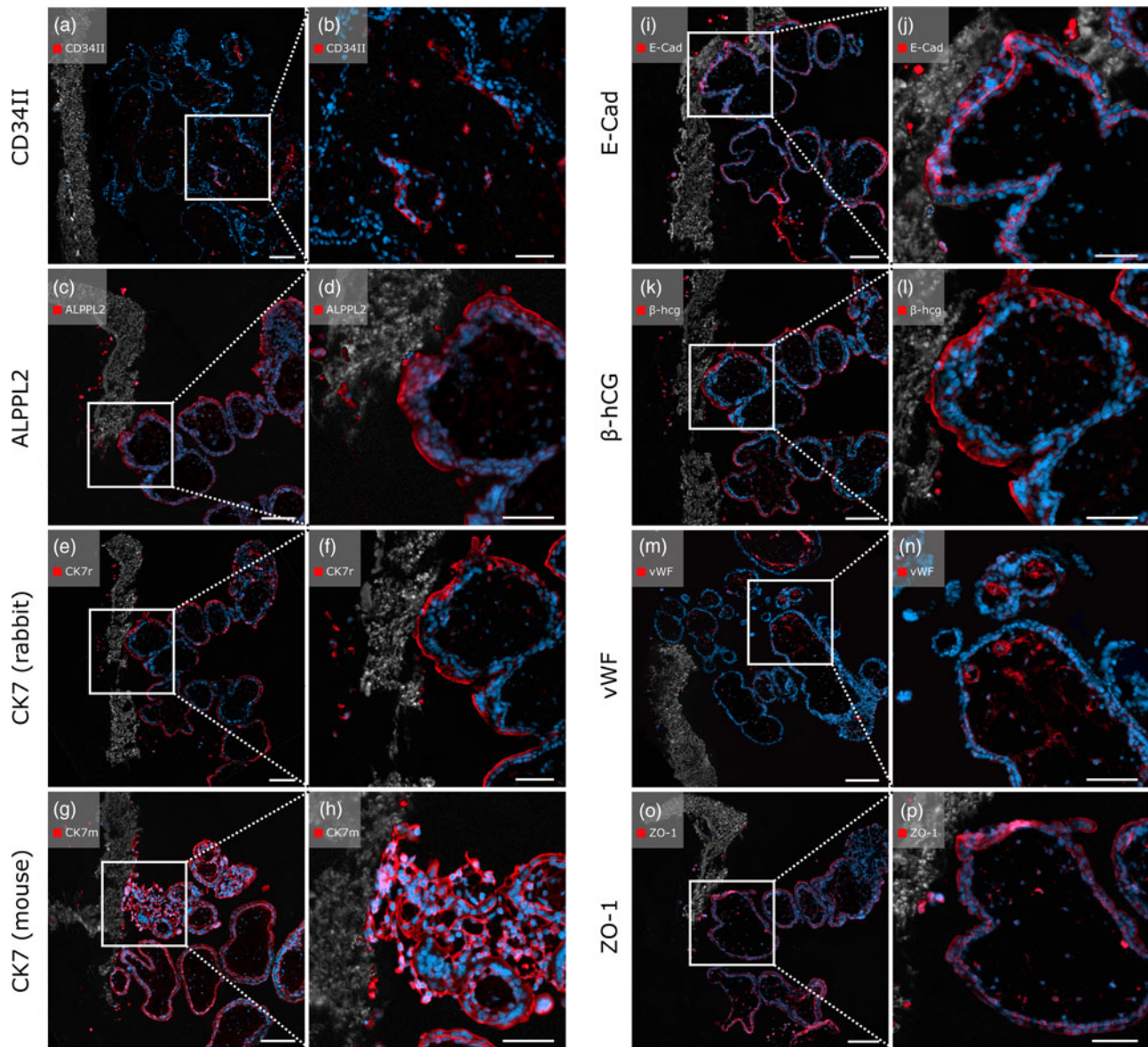


Fig. 6. Immunofluorescent staining with placenta-relevant antibodies on first trimester placental villi attached to heat-sensitive PCL/PLA scaffolds after pepsin digestion. White boxes indicate the zoom-in area on the right image side. All antibodies tested showed specific fluorescence signals. Scale bars in (a,c,e,g,i) represent 100 μm , and those in (b,d,f,h,j) represent 50 μm .

fluorescent signal intensities over large image areas and compared the results with conventional qualitative histological analysis methods. In contrast to qualitative histological examinations usually evaluated by an individual (Honig et al., 2005), the major advantage of automated computational analysis is a more objective and therefore less biased interpretation of data (Nezami & Butcher, 2000; Fantuzzo et al., 2017). Our quantitative evaluation allows for a more precise description of immunostaining as it is based on large portions of the tissue compared to small sections, which are often used in conventional quantitative analyzed histological studies.

One purpose of antigen retrieval is to reveal epitopes and other cellular targets (Robinson & Vandr , 2001). This is necessary because tissue samples are generally fixed prior to histological processing. Fixation preserves the biological material as close as possible to its natural state (Robinson & Vandr , 2001), since primary and secondary protein structures are cross-linked (Mason & O'Leary, 1991). However, sample fixation significantly reduces the

immunoreactivity of most antigens (Battifora & Kopinski, 1986; Leong & Gilham, 1989).

With the successful implementation of a comprehensive, automated quantitative image analysis pipeline, we identified the optimal pretreatment for selected placenta-relevant antibodies. Our approach allowed for a direct comparison of the effects of different antigen retrieval pretreatments on immunostaining specificity and intensity. While each antibody showed specific fluorescence signals after heat-induced antigen retrieval; however, not all markers displayed positive staining after proteolytic digestion with pepsin, e.g. nonspecific staining was observed with CD163. We assume that this is due to incomplete degradation of cross-links, as nonspecific primary antibody binding may occur in the presence of unreacted hydroxymethyl groups after formaldehyde fixation. Additionally, depending on the type of epitope and marker, nonspecific interactions may occur between the primary antibody and other antigens within the tissue (Daneshtalab

et al., 2010). No staining was observed with eight of the antibodies after pepsin digestion, indicating that their epitopes may have been completely degraded. This closely parallels findings by Battifora and Kopinski (1986) and Daneshtalab et al. (2010), who argued that overdigestion damages the morphology and immunoreactivity of tissue and may reduce the number of antigenic sites available for immunostaining. We speculate that the threshold for overdigestion varies and depends not only on the duration of fixation but also on the marker and the type of tissue examined. As such, this must be empirically determined for each antibody. It is possible that shortening the digestion time for antibodies not showing immunostaining signals using proteolytic antigen retrieval would yield positive results. These speculations are consistent with other research groups (Daneshtalab et al., 2010).

To exclude nonspecific staining due to enzymatic or heat-induced antigen retrieval, we performed antibody staining on first trimester placenta cryosections as an additional verification method. As cryosections enable immunostaining without antigen retrieval techniques, the occurrence or loss of nonspecific antigenicity is unlikely (Hira et al., 2019). This approach thus provides a valid method verifying specificity of the antibodies used in this publication, besides a comprehensive literature study to determine whether relevant morphological structures are expressed in first trimester placental tissue (MacNeil et al., 2020). However, the tissue morphology of snap-frozen placenta samples was of inferior morphological quality compared to paraffin-embedded samples due to the freezing procedure (Blaschitz et al., 2008). Thus, the requirements of tissue conservation through fixation and the preservation of antigenicity in immunostaining constantly conflict. Nevertheless, accurate identification of immunostaining on cryosections was possible. All antibodies showed positive staining in the expected morphological areas. The comparison of the immunostaining on untreated cryosections with the staining on heat- or enzyme-treated paraffin sections revealed that all antibodies bind specifically in the expected regions. In the case of CD163, comparison with staining on cryosections again demonstrated that immunostaining after pepsin digestion results in nonspecific binding.

To further ensure antibody specificity, monoclonal antibodies should be preferred, as they bind to a single, definable epitope on the target antigen and are highly specific and consistent between experiments (MacNeil et al., 2020). Thus, in the present study, 11 of the 17 antibodies investigated derived from monoclonal origins.

Our study was supplemented by a qualitative analysis which revealed that the cell type-specific staining for each antibody depends on the applied antigen retrieval method, as observed for β -hCG and both anti-CK7 antibodies. Based on that observation, it is important to relate signal intensities to cell type-specific staining efficiency. For example, high fluorescence intensity levels in quantitative analysis either can occur as high-intensity signal originating from one cell type, or are a result of accumulating signal intensities based on staining of multiple, different cell types. Thus, the qualitative aspect should always be considered before interpreting quantitative image analysis to avoid the misinterpretation of fluorescence signals. This highlights an important limitation of computer-based image quantification. While artificial intelligence and deep-learning systems have revolutionized global pathology in the primary diagnosis of certain cancer cell types, computational algorithms in other histological fields, especially in unsupervised architectures, are prone to misinterpreting artifacts as true biological signals. Important quality parameters that matter can be inconspicuous and easily overlooked (Evans et al., 2017; Tomaszewski, 2021).

Nevertheless, quantification in histology and thereby standardized quantitative automated image analysis are becoming increasingly important in the diagnosis of placenta-associated diseases. In addition to studies dealing with the semi-quantitative evaluation of syncytial knots to investigate placental malfunction (Senagore et al., 2016; Kidron et al., 2017; Parks, 2019), the quantification of the vessel number and layer composition during uterine and placental vascularization, for instance, is of great importance for diagnosing pathologies such as preeclampsia or intrauterine growth restriction. Up to now, the visualization of placental vascularization is mainly performed using 3D ultrasound technology (Campbell, 2007), which has limited precision in depicting the histological composition of vessel layers. As a result, important information at a cellular level remains unknown. To generate further knowledge regarding these pregnancy-associated diseases, automated quantitative image analysis based on immunostained placental sections using markers such as desmin, vimentin, and SMA for vascular detection, as described in this study, might provide valuable insights. Beyond that, the evaluated antibodies offer the possibility for further placenta-related histological investigations on a quantitative level, such as trophoblast invasion by using the trophoblast markers HLA-G, CK7, and β -hCG or the examination of maternal and childhood obesity via ALPPL2 and leptin antibodies (Hirschmugl et al., 2018).

Automated quantitative image analysis is a powerful technique minimizing operator error and biased interpretation; however, the qualitative assessment of antibody binding remains essential to properly assess immunofluorescence specificity and to avoid misinterpreting the data (Nezami & Butcher, 2000; Gertych et al., 2015). Hence, in our opinion, the qualitative analysis of each antibody enables the optimization of quantitative analysis methods and thus the possibility of objective diagnostic procedures.

In addition, our automated quantitative image analysis approach enabled a direct assessment of whether pepsin digestion can serve as an alternative to conventional antigen retrieval pretreatment methods for thermo-sensitive scaffold-based placental cell culture systems. Proteolytic digestion with pepsin expands on a recently described method enabling antigen retrieval of thermo-sensitive specimens as an alternative to common heat-induced methods (Ramos-Vara and Beissenherz, 2000; Fuchs et al., 2018). Our evaluation demonstrated that 8 out of 17 investigated placenta-relevant antibodies showed positive immunostaining after pepsin digestion, making the enzymatic method a heatless antigen retrieval alternative for these antibodies. These investigations can help in finding suitable new *in vitro* models for placental research that are comparable to the *in vivo* situation.

There is a clear need for a quantitative image-based assessment of antibodies in placental research as considerable knowledge about placental pathologies occurring in the first and second trimesters of pregnancy is mainly gained from *in vitro* studies using immunostaining assays (Aengenheister et al., 2018; Turco et al., 2018; Knöfler et al., 2019). In addition, the ability to compare placental cell culture models with the *in vivo* placenta situation illustrates a major benefit of the present study. Hence, our evaluation serves as a powerful tool for the selection of antibody and pretreatment to be used in implantation and placental research to provide objective and precise results.

Conclusion

The presented evaluation of selected antigen retrieval methods for 17 placenta-relevant antibodies serves as a helpful tool in

placentation and implantation diagnostic and research. Automated quantitative image analysis supports the unbiased interpretation of large tissue areas; however, the qualitative assessment of each antibody has to be considered. Hence, our findings provide the potential for further progress in the development of placenta cell culture models and thus the clarification of pregnancy-associated diseases.

Supplementary material. To view supplementary material for this article, please visit <https://doi.org/10.1017/S1431927621012630>.

Acknowledgment. We thank Dr. Andreas Glasner for recruiting first trimester placental tissue samples for this study. This research was funded in whole by the Austrian Science Fund (FWF) and Christian Doppler Research Association (CDG): PIR7-B28. For the purpose of open access, the author has applied a CC BY public copyright license to any Author Accepted Manuscript version arising from this submission.

Author contributions statement. J.F. designed and performed the experiments, analyzed the data, and wrote the manuscript. O.N. designed the experiments and edited the text. C.D. performed the experiments and provided technical assistance. S.G., G.M., LL.-O., and M.G. provided technical assistance and edited the text. D.B. wrote the manuscript and edited the text. All authors read and approved the final manuscript, and read and met the ICMJE criteria for authorship.

Conflict of interest. The authors declare no conflict of interest.

References

- Aengenheister L, Keevend K, Muoth C, Schönenberger R, Diener L, Wick P & Buerki-Thurnherr T (2018). An advanced human in vitro co-culture model for translocation studies across the placental barrier. *Sci Rep* **8**(1), 5388. doi:10.1038/s41598-018-23410-6
- Battifora H & Kopinski M (1986). The influence of protease digestion and duration of fixation on the immunostaining of keratins. A comparison of formalin and ethanol fixation. *J Histochem Cytochem* **34**(8), 1095–1100. doi:10.1177/34.8.2426335
- Blaschitz A, Gauster M & Dohr G (2008). Application of cryo-compatible antibodies to human placenta paraffin sections. *Histochem Cell Biol* **130**(3), 595–599. doi:10.1007/s00418-008-0458-z
- Böckle BC, Sölder E, Kind S, Romani N & Sepp NT (2008). DC-sign+ CD163+ macrophages expressing hyaluronan receptor LYVE-1 are located within chorion villi of the placenta. *Placenta* **29**(2), 187–192. doi:10.1016/j.placenta.2007.11.003
- Campbell S (2007). Placental vasculature as visualized by 3D power Doppler angiography and 3D color Doppler imaging. *Ultrasound Obstet Gynecol* **30**(6), 917–920. doi:10.1002/uog.5195
- Daneshtalab N, Doré JJE & Smeda JS (2010). Troubleshooting tissue specificity and antibody selection: Procedures in immunohistochemical studies. *J Pharmacol Toxicol Methods* **61**(2), 127–135. doi:10.1016/j.vascn.2009.12.002
- Evans AJ, Salama ME, Henricks WH & Pantanowitz L (2017). Implementation of whole slide imaging for clinical purposes: Issues to consider from the perspective of early adopters. *Arch Pathol Lab Med* **141**(7), 944–959. doi:10.5858/arpa.2016-0074-OA
- Fantuzzo JA, Mirabella VR, Hamod AH, Hart RP, Zahn JD & Pang ZP (2017). Intellicount: High-throughput quantification of fluorescent synaptic protein puncta by machine learning. *eNeuro* **4**(6). doi:10.1523/ENEURO.0219-17.2017.
- Fuchs J, Mueller M, Daxböck C, Stückler M, Lang I, Leitinger G, Bock E, El-Heliebi A, Moser G, Glasmacher B & Brislinger D (2018). Histological processing of un-/cellularized thermosensitive electrospun scaffolds. *Histochem Cell Biol*. doi:10.1007/s00418-018-1757-7.
- Gauster M, Siwet M & Huppertz B (2009). Fusion of villous trophoblast can be visualized by localizing active caspase 8. *Placenta* **30**(6), 547–550. doi:10.1016/j.placenta.2009.03.007
- Gertych A, Ing N, Ma Z, Fuchs TJ, Salman S, Mohanty S, Bhele S, Velásquez-Vacca A, Amin MB & Knudsen BS (2015). Machine learning approaches to analyze histological images of tissues from radical prostatectomies. *Comput Med Imaging Graph* **46**(Pt 2), 197–208. doi:10.1016/j.compmedimag.2015.08.002
- Guettler J, Forstner D, Cvirn G, Maninger S, Brugger BA, Nonn O, Kupper N, Pritz E, Wernitznig S, Dohr G, Hutter H, Juch H, Isermann B, Kohli S & Gauster M (2021). Maternal platelets pass interstices of trophoblast columns and are not activated by HLA-G in early human pregnancy. *J Reprod Immunol* **144**, 103280. doi:10.1016/j.jri.2021.103280
- Gurcan MN, Boucheron LE, Can A, Madabhushi A, Rajpoot NM & Yener B (2009). Histopathological image analysis: A review. *IEEE Rev Biomed Eng* **2**, 147–171. doi:10.1109/RBME.2009.2034865
- Haider S, Meinhardt G, Saleh L, Kunihs V, Gamperl M, Kaindl U, Ellinger A, Burkard TR, Fiala C, Pollheimer J, Mendjan S, Latos PA & Knöfler M (2018). Self-Renewing trophoblast organoids recapitulate the developmental program of the early human placenta. *Stem Cell Rep* **11**(2), 537–551. doi:10.1016/j.stemcr.2018.07.004
- Hidden U, Wadsack C, Prutsch N, Gauster M, Weiss U, Frank H-G, Schmitz U, Fast-Hirsch C, Hengstschläger M, Pötgens A, Rübén A, Knöfler M, Haslinger P, Huppertz B, Bilban M, Kaufmann P & Desoye G (2007). The first trimester human trophoblast cell line ACH-3P: A novel tool to study autocrine/paracrine regulatory loops of human trophoblast subpopulations—TNF- α stimulates MMP15 expression. *BMC Dev Biol* **7**, 137. doi:10.1186/1471-213X-7-137
- Higgins C (2015). Applications and challenges of digital pathology and whole slide imaging. *Biotech Histochem* **90**(5), 341–347. doi:10.3109/10520295.2015.1044566
- Hira VVV, Jong ALd, Ferro K, Khurshed M, Molenaar RJ & van Noorden CJF (2019). Comparison of different methodologies and cryostat versus paraffin sections for chromogenic immunohistochemistry. *Acta Histochem* **121**(2), S. 125–S. 134. doi:10.1016/j.acthis.2018.10.011
- Hirschmugl B, Crozier S, Matthews N, Kitzinger E, Klymiuk I, Inskip HM, Harvey NC, Cooper C, Sibley CP, Glazier J, Wadsack C, Godfrey KM, Desoye G & Lewis RM (2018). Relation of placental alkaline phosphatase expression in human term placenta with maternal and offspring fat mass. *Int J Obes* **42**(6), 1202–1210. doi:10.1038/s41366-018-0136-8
- Honig A, Rieger L, Kapp M, Dietl J & Kämmerer U (2005). Immunohistochemistry in human placental tissue—Pitfalls of antigen detection. *J Histochem Cytochem* **53**(11), 1413–1420. doi:10.1369/jhc.5A6664.2005
- Kacemi A, Vervelle C, Uzan S & Challier JC (1999). Immunostaining of vascular, perivascular cells and stromal components in human placental villi. *Cell Mol Biol* **45**(1), 101–113.
- Kidron D, Vainer I, Fisher Y & Sharony R (2017). Automated image analysis of placental villi and syncytial knots in histological sections. *Placenta* **53**, 113–118. doi:10.1016/j.placenta.2017.04.004
- Kim S-W, Roh J & Park C-S (2016). Immunohistochemistry for pathologists: Protocols, pitfalls, and tips. *J Pathol Transl Med* **50**(6), 411–418. doi:10.4132/jptm.2016.08.08
- Knöfler M, Haider S, Saleh L, Pollheimer J, Gamage TKJB & James J (2019). Human placenta and trophoblast development: Key molecular mechanisms and model systems. *Cell Mol Life Sci* **76**(18), 3479–3496. doi:10.1007/s00018-019-03104-6
- Kreuder A-E, Bolaños-Rosales A, Palmer C, Thomas A, Geiger M-A, Lam T, Amler A-K, Markert UR, Lauster R & Kloke L (2020). Inspired by the human placenta: A novel 3D bioprinted membrane system to create barrier models. *Sci Rep* **10**(1), 15606. doi:10.1038/s41598-020-72559-6
- Lanoix D, St-Pierre J, Lacasse AA, Viau M, Lafond J & Vaillancourt C (2012). Stability of reference proteins in human placenta: General protein stains are the benchmark. *Placenta* **33**(3), 151–156. doi:10.1016/j.placenta.2011.12.008
- Leong AS & Gilham PN (1989). The effects of progressive formaldehyde fixation on the preservation of tissue antigens. *Pathology* **21**(4), 266–268.
- Liu C, Ge M, Ma J, Zhang Y, Zhao Y & Cui T (2019). Homeobox A10 promotes the proliferation and invasion of bladder cancer cells via regulation of matrix metalloproteinase-3. *Oncol Lett* **18**(1), 49–56. doi:10.3892/ol.2019.10312
- Londero AP, Orsaria M, Grassi T, Calcagno A, Marzinotto S, Ceraudo M, Fruscalzo A, Driul L & Mariuzzi L (2013). Placental hCG

- immunohistochemistry and serum free-Beta-hCG at 11-13 weeks' gestation in intrauterine fetal demise. *Histochem Cell Biol* **139**(4), 595–603. doi:10.1007/s00418-012-1054-9
- MacNeil T, Vathiotis IA, Martinez-Morilla S, Yaghoobi V, Zugazagoitia J, Liu Y & Rimm DL** (2020). Antibody validation for protein expression on tissue slides: A protocol for immunohistochemistry. *BioTechniques* **69**(6), S. 460–S. 468. doi:10.2144/btn-2020-0095
- Marzioni D, Banita M, Felici A, Paradinas FJ, Newlands E, Nictolis Md, Mühlhauser J & Castellucci M** (2001). Expression of ZO-1 and occludin in normal human placenta and in hydatidiform moles. *Mol Hum Reprod* **7**(3), 279–285. doi:10.1093/molehr/7.3.279
- Mason JT & O'Leary TJ** (1991). Effects of formaldehyde fixation on protein secondary structure: A calorimetric and infrared spectroscopic investigation. *J Histochem Cytochem* **39**(2), 225–229. doi:10.1177/39.2.1987266
- McQuin C, Goodman A, Chernyshev V, Kamentsky L, Cimini BA, Karhohs KW, Doan M, Ding L, Rafelski SM, Thirstrup D, Wiegreae W, Singh S, Becker T, Caicedo JC & Carpenter AE** (2018). CellProfiler 3.0: Next-generation image processing for biology. *PLoS Biol* **16**(7), e2005970. doi:10.1371/journal.pbio.2005970
- Motulsky HJ & Brown RE** (2006). Detecting outliers when fitting data with nonlinear regression: A new method based on robust nonlinear regression and the false discovery rate. *BMC Bioinformatics* **7**, 123. doi:10.1186/1471-2105-7-123
- Nezami E & Butcher JN** (2000). Objective Personality Assessment. In *Handbook of Psychological Assessment (Third Edition)*, Golstein Gerald & Hersen Michel (Eds.), (Third Edition). pp. 413–435. Oxford, UK: Elsevier. <https://doi.org/10.1016/B978-008043645-6/50094-X>
- Nuovo G** (2006). The utility of immunohistochemistry and In situ hybridization in placental pathology. *Arch Path Lab Med* **130**(7), 979–983. doi:10.5858/2006-130-979-TUOIAI
- Ohyama M, Itani Y, Yamanaka M, Goto A, Kato K, Ijiri R & Tanaka Y** (2004). Maternal, neonatal, and placental features associated with diffuse chorioamniotic hemosiderosis, with special reference to neonatal morbidity and mortality. *Pediatrics* **113**(4), 800–805. doi:10.1542/peds.113.4.800
- Parks WT** (2019). Increased syncytial knot formation. In *Pathology of the Placenta*, Yee Khong T, Mooney EE, Nikkels PGJ, Morgan TK & Gordijn SJ (Eds.), pp. 131–137. Cham: Springer International Publishing.
- Pemathilaka RL, Reynolds DE & Hashemi NN** (2019). Drug transport across the human placenta: Review of placenta-on-a-chip and previous approaches. *Interface Focus* **9**(5), 20190031. doi:10.1098/rsfs.2019.0031
- Ramos-Vara José A & Beissenherz Marilyn E.** (2000). Optimization of Immunohistochemical Methods using two Different Antigen Retrieval Methods on Formalin-Fixed, Paraffin-Embedded Tissues: Experience with 63 Markers. *Journal of Veterinary Diagnostic Investigation* **12**(4), 307–311. doi: <http://dx.doi.org/10.1177/104063870001200402>
- Riordan DP, Varma S, West RB & Brown PO** (2015). Automated analysis and classification of histological tissue features by multi-dimensional microscopic molecular profiling. *PLoS One* **10**(7). doi:10.1371/journal.pone.0128975.
- Robinson JM & Vandré DD** (2001). Antigen retrieval in cells and tissues: Enhancement with sodium dodecyl sulfate. *Histochem Cell Biol* **116**(2), 119–130. doi:10.1007/s004180100299
- Roescher AM, Timmer A, Erwich JJHM & Bos AF** (2014). Placental pathology, perinatal death, neonatal outcome, and neurological development: A systematic review. *PLoS One* **9**(2), e89419. doi:10.1371/journal.pone.0089419
- Sati L, Seval Y, Yasemin Demir A, Kosanek G, Kohnen G & Demir R** (2007). Cellular diversity of human placental stem villi: An ultrastructural and immunohistochemical study. *Acta Histochem* **109**(6), 468–479. doi:10.1016/j.acthis.2007.04.006
- Senagore PK, Holzman CB, Parks WT & Catov JM** (2016). Working towards a reproducible method for quantifying placental syncytial knots. *Pediatr Dev Pathol* **19**(5), 389–400. doi:10.2350/15-08-1701-OA.1
- Silva JF & Serakides R** (2016). Intrauterine trophoblast migration: A comparative view of humans and rodents. *Cell Adh Migr* **10**(1–2), 88–110. doi:10.1080/19336918.2015.1120397
- Tomaszewski JE** (2021). Overview of the role of artificial intelligence in pathology: The computer as a pathology digital assistant. In *Artificial Intelligence and Deep Learning in Pathology*, Cohen Stanley (Ed.), 1st Edition. pp. 237–262. Philadelphia: Elsevier.
- Tsai P-JS, Davis J & Bryant-Greenwood G** (2015). Systemic and placental leptin and its receptors in pregnancies associated with obesity. *Reprod Sci* **22**(2), 189–197. doi:10.1177/1933719114537718
- Turco MY, Gardner L, Kay RG, Hamilton RS, Prater M, Hollinshead MS, McWhinnie A, Esposito L, Fernando R, Skelton H, Reimann F, Gribble FM, Sharkey A, Marsh SGE, O'Rahilly S, Hemberger M, Burton GJ & Moffett A** (2018). Trophoblast organoids as a model for maternal-fetal interactions during human placentation. *Nature* **564**(7735), 263–267. doi:10.1038/s41586-018-0753-3
- Vonbrunn E, Mueller M, Pichlsberger M, Sundl M, Helmer A, Wallner SA, Rinner B, Tuca A-C, Kamolz L-P, Brislinger D, Glasmacher B & Lang-Olip I** (2020). Electrospun PCL/PLA scaffolds are more suitable carriers of placental mesenchymal stromal cells than collagen/elastin scaffolds and prevent wound contraction in a mouse model of wound healing. *Front Bioeng Biotechnol* **8**, 604123. doi:10.3389/fbioe.2020.604123
- Weibrecht I, Lundin E, Kiflemariam S, Mignardi M, Grundberg I, Larsson C, Koos B, Nilsson M & Söderberg O** (2013). In situ detection of individual mRNA molecules and protein complexes or post-translational modifications using padlock probes combined with the in situ proximity ligation assay. *Nat Protoc* **8**(2), 355–372. doi:10.1038/nprot.2013.006